Materials Letters 207 (2017) 8–11

Contents lists available at ScienceDirect

Materials Letters

journal homepage: www.elsevier.com/locate/mlblue

BiOI/α–$AgAl_{0.4}Ga_{0.6}O_2$ heterostructures with controllable visible–light absorption and enhanced carrier separation efficiency

Maocai Zhang, Chen Tian, Lingyan Dang, Shifeng Zhao, Qingshan Lu *

School of Physical Science and Technology and Inner Mongolia Key Laboratory of Nanoscience & Nanotechnology, Inner Mongolia University, Hohhot 010021, China

ARTICLE INFO

Article history:
Received 23 May 2017
Received in revised form 26 June 2017
Accepted 5 July 2017
Available online 6 July 2017

Keywords:
Composite materials
Heterojunction
Microstructure
Band gap

ABSTRACT

BiOI/α–$AgAl_{0.4}Ga_{0.6}O_2$ heterostructures are synthesized by a precipitation route. The results show that flower–like BiOI microspheres grow on platelet–like α–$AgAl_{0.4}Ga_{0.6}O_2$. With regard to the heterojunctions, the visible–light absorption edges expand from 470 to 650 nm by controlling the ratio of α–$AgAl_{0.4}Ga_{0.6}O_2$ to BiOI. Photoluminescence spectra demonstrate that the BiOI/α–$AgAl_{0.4}Ga_{0.6}O_2$ exhibits lower emission intensity than the BiOI and α–$AgAl_{0.4}Ga_{0.6}O_2$, indicating the enhancement of carrier separation efficiency which is also verified by electrochemical impedance spectroscopy. Thus, the BiOI/α–$AgAl_{0.4}Ga_{0.6}O_2$ heterostructures can efficiently utilize visible light and facilitate carrier separation.

1. Introduction

Semiconductor photocatalysis has been regarded as a promising technology for environmental purification [1,2]. In order to efficiently utilize solar light, considerable researches are focused on the development of visible–light–responsive and efficient photocatalysts [3,4]. Concerning the drawbacks of traditional photocatalysts with large band gap and low photocatalytic efficiency, various modifications including ions doping [5], dye sensitization [6], semiconductor coupling [7] and heterostructure [8] have been proposed to overcome the issues. Especially, the design of semiconductor heterostructures is an effective strategy for improving photocatalytic efficiency [9].

BiOI with narrow band gap shows visible–light response [10]. Yosefi and co–workers design the p–BiOI/n–$ZnFe_2O_4$ heterostructures to remove the acid orange 7 from wastewater [11]. Yu et al. prepare Pt/BiOI nanoplate to form Schottky–type heterojunctions and study the degradation of acid orange II under visible light [12]. However, BiOI still suffers from weak photooxidation ability and high recombination rate. Solid solution α–$AgAl_{0.4}Ga_{0.6}O_2$ displays visible–light activity and strong oxidization ability [13]. Thus, on the purpose of achieving high photocatalytic activity, the design and fabrication of the heterostructures become very significant. In this work, BiOI/α–$AgAl_{0.4}Ga_{0.6}O_2$ heterostructures consisting of platelet α–$AgAl_{0.4}Ga_{0.6}O_2$ decorated with BiOI microspheres are prepared by precipitation method. The UV–vis absorption behavior of the BiOI/α–$AgAl_{0.4}Ga_{0.6}O_2$ proves the efficient utilization of visible light. The heterojunctions facilitate the separation of photogenerated carriers.

2. Experimental section

Pure α–$AgAl_{0.4}Ga_{0.6}O_2$ was synthesized as follows: 1.0 g of β–$AgAl_{0.4}Ga_{0.6}O_2$ was dispersed into deionized water under stirring, then transferred into a Teflon–lined stainless autoclave and kept at 100 °C for 15 h. The α–$AgAl_{0.4}Ga_{0.6}O_2$ was obtained. BiOI/α–$AgAl_{0.4}Ga_{0.6}O_2$ heterostructures were prepared by precipitation method. Different amounts of α–$AgAl_{0.4}Ga_{0.6}O_2$ were dispersed into the solution of deionized water (60 mL) and 60 mL of ethylene glycol containing 2 mmol of $Bi(NO_3)_3 \cdot 5H_2O$. 2 mmol of KI dissolved in deionized water (20 mL) was added to the α–$AgAl_{0.4}Ga_{0.6}O_2$ suspension. After stirring for 5 h, the products were washed and dried at 60 °C for 10 h. Then X%BiOI/α–$AgAl_{0.4}Ga_{0.6}O_2$ was obtained and X represented the molar ratio of BiOI to α–$AgAl_{0.4}Ga_{0.6}O_2$.

Phase structure was investigated on PANalytical Empyrean X–ray diffractometer using Cu K_α radiation. Morphology was characterized by a Hitachi S–4800 scanning electron microscopy (SEM). Microstructure analysis was carried out with a JEM-2010 transmission electron microscope (TEM). UV–visible absorption (UV–vis) and photoluminescence (PL) spectra were obtained using Hitachi U–3900 and Hitachi F–7000 spectrophotometers, respectively. The excitation wavelength is 280 nm. Electrochemical impedance spectroscopy (EIS) was conducted on a CHI–660E electrochemical system with a three–electrode cell and 0.1 M Na_2SO_4 as the electrolyte.

* Corresponding author.
E-mail address: luqs@imu.edu.cn (Q. Lu).

http://dx.doi.org/10.1016/j.matlet.2017.07.037

3. Results and discussion

Fig. 1a shows the XRD patterns of samples. The α–$AgAl_{0.4}Ga_{0.6}O_2$ exhibits sharp diffraction peaks, indicating its pure phase and well crystallinity. For BiOI, four peaks match with the (1 0 2), (1 1 0), (2 0 0) and (2 1 2) crystal planes belonging to single phase of tetragonal structure [11]. Diffraction peaks attributed to BiOI and α–$AgAl_{0.4}Ga_{0.6}O_2$ are observed, revealing the coexistence of BiOI and α–$AgAl_{0.4}Ga_{0.6}O_2$ phases for BiOI/α–$AgAl_{0.4}Ga_{0.6}O_2$. In addition, neither impurity nor secondary phases are detected, suggesting the successful fabrication of pure BiOI/α–$AgAl_{0.4}Ga_{0.6}O_2$.

To obtain detailed morphologies of particle, the samples were characterized by SEM. As shown in Fig. 1b, it can be seen that pure BiOI demonstrates flower–like microspheres with a diameter of about 1–2.4 μm. These particles keep hierarchical structures which are composed of high density nanosheets. Differently, α–$AgAl_{0.4}Ga_{0.6}O_2$ possesses a platelet–like structure with a discrepant diameter shown in Fig. 1c. That is to say, BiOI is easily shaped into microspheres, while the shape of α–$AgAl_{0.4}Ga_{0.6}O_2$ tends to be platelet [3,13]. SEM image of 0.67BiOI/α–$AgAl_{0.4}Ga_{0.6}O_2$ is shown in Fig. 1d. It is obvious that the mixed morphology includes platelet–like and flower–like microsphere structures. With the increase of the molar ratio of α–$AgAl_{0.4}Ga_{0.6}O_2$ in the composites, the morphology has inverted from flower–like microspheres into platelets, which may suggest that the BiOI are deposited on the surface of the α–$AgAl_{0.4}Ga_{0.6}O_2$ platelets. The SEM results confirm the coexistence of BiOI and α–$AgAl_{0.4}Ga_{0.6}O_2$.

Fig. 2 shows the TEM micrographs of the BiOI/α–$AgAl_{0.4}Ga_{0.6}O_2$. The presence of the microspheres and platelet particles (Fig. 2a) confirms the presence of BiOI and α–$AgAl_{0.4}Ga_{0.6}O_2$ in the composites. This result is in accordance with the SEM analysis. For BiOI/α–$AgAl_{0.4}Ga_{0.6}O_2$, the phase of BiOI and α–$AgAl_{0.4}Ga_{0.6}O_2$ are distinct in the sample (Fig. 2b). The high resolution image of the 0.67BiOI/α–$AgAl_{0.4}Ga_{0.6}O_2$ is illustrated in Fig. 2c. It is evident that there are two sets of lattice fringes in the pattern. The distance of the lattice fringes is about 0.3055 nm, being close to the interplanar spacing of the (0 0 4) plane for α–$AgAl_{0.4}Ga_{0.6}O_2$. The distance of the lattice fringes is 0.3011 nm matching well with the interplanar spacing of the (1 0 2) plane for BiOI. In addition, the lattice fringes corresponding to the (1 0 5) plane of 0.1750 nm for α–$AgAl_{0.4}Ga_{0.6}O_2$ is also observed. The HRTEM results prove that the obtained sample consists of BiOI and α–$AgAl_{0.4}Ga_{0.6}O_2$ and the BiOI/α–$AgAl_{0.4}Ga_{0.6}O_2$ heterostructures are successfully formed. This evidence strongly demonstrates that the flower–like microsphere BiOI acting as the shell are assembled on the surface of the α–$AgAl_{0.4}Ga_{0.6}O_2$.

Fig. 3a shows the UV–vis absorption spectra of the samples. The absorption edges of the BiOI and the α–$AgAl_{0.4}Ga_{0.6}O_2$ locate at about 650 and 470 nm, respectively. The cut–off absorption wavelength of 650 nm for BiOI is larger than 470 nm of α–$AgAl_{0.4}Ga_{0.6}O_2$. The BiOI/α–$AgAl_{0.4}Ga_{0.6}O_2$ exhibits good visible light absorption ability. Compared with α–$AgAl_{0.4}Ga_{0.6}O_2$, a red shift of the absorption edge of the BiOI/α–$AgAl_{0.4}Ga_{0.6}O_2$ is observed in the UV–vis absorption spectrum with the increase of BiOI molar ratio.

Optical band gap can be determined according to the Tauc's law [14,15]. In this study, the formula is expressed as $(\alpha h\nu)^{1/2} = A\,(h\nu - E_g)$, because BiOI and α–$AgAl_{0.4}Ga_{0.6}O_2$ are indirect semiconductors [13,16]. As shown in Fig. 3b, the tangents of the lines are extrapolated to zero to obtain the band gap E_g. The E_g of α–$AgAl_{0.4}Ga_{0.6}O_2$

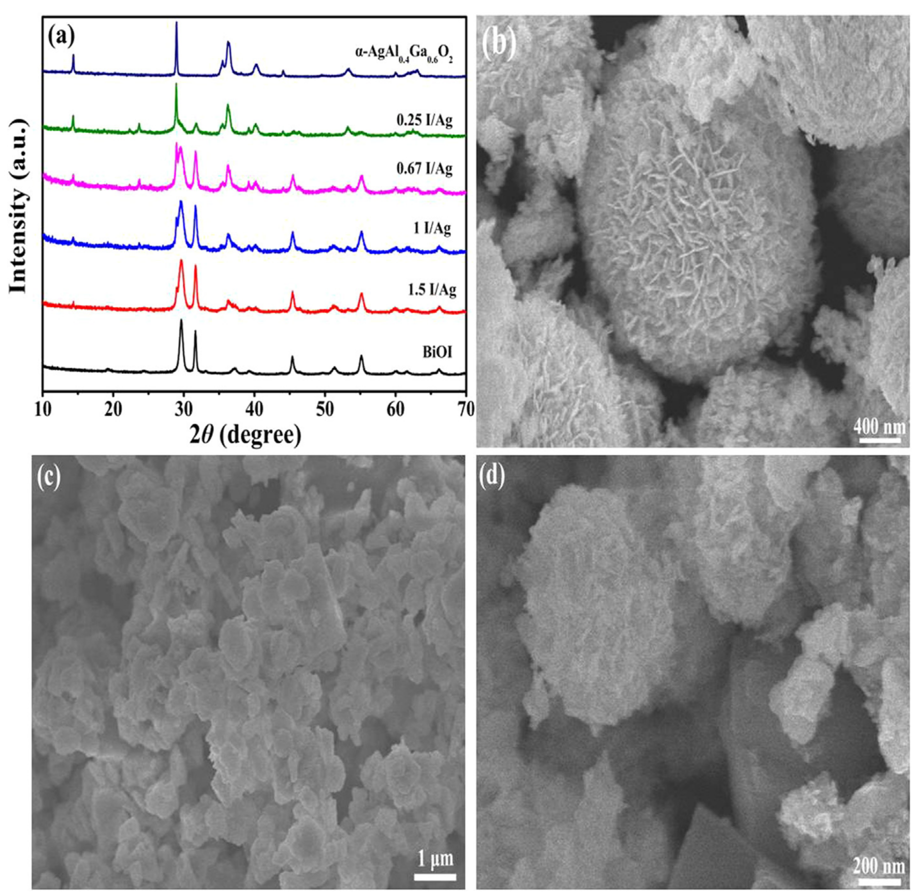

Fig. 1. XRD patterns of BiOI, X%BiOI/α–$AgAl_{0.4}Ga_{0.6}O_2$ and α–$AgAl_{0.4}Ga_{0.6}O_2$ (a); SEM images of BiOI (b), α–$AgAl_{0.4}Ga_{0.6}O_2$ (c) and 0.67BiOI/α–$AgAl_{0.4}Ga_{0.6}O_2$ (d).